Supplementary Information (SI) for ChemComm.
This journal is © The Royal Society of Chemistry 2026

Supplementary Information for

GeAsP: a new two-dimensional layered material for highly efficient photocatalytic CO_2 reduction

Jiaqi Song[a], Qingwei Wang[a,b,c], Yong Ke[a,b,c], Yunyan Wang[a,b,c], Yun Li[a,b,c], Yanjie Liang[a,b,c], Feiping Zhao[a,b,c], Xiaoyu Huang[a], Xiaobo Min[a,b,c*], Liyuan Chai[a,b,c], Cong Peng[a,b,c*]

[a] School of Metallurgy and Environment, Central South University, Changsha 410083 China;

[b] State Key Laboratory of Advanced Metallurgy for Non-ferrous Metals, Changsha 410083 China;

[c] Chinese National Engineering Research Center for Control & Treatment of Heavy Metal Pollution, Changsha 410083 China

***Corresponding author**: pengcong0704@csu.edu.cn; mxb@csu.edu.cn*

1. Synthesis of GeAsP crystal

Bulk GeAsP crystals were synthesized using the CVT method. Briefly, a mixture of gray arsenic (99.9999%, particles), red phosphorus (99.999%, blocks), germanium (99.999%, particles) and idine (99.5%, powder, used as a transport agent) was placed on the sealing end of a quartz tube. After being pumped to high vacuum, the end of the quartz tube were sealed, and the quartz tube was horizontally placed in a tube furnace with two independent heating zones (The length ratio is 1:1). The quartz tube was then heated up to 850°C-800°C-850°C for 1 h, held at this temperature for 6-8 h, then cooled to 100°C-300°C-100°C for 2 h, and finally cooled to room temperature.

2. Preparation of GeAsP/g-C_3N_4 heterostructure

Before exfoliating, the GeAsP crystal was homogenized by grinding it in an agate mortar in a glove box (under Ar atmosphere). Then, 1-50 mg of GeAsP and 100 mg of g-C_3N_4 (purchased from XFNANO) were mixed and added to 45 ml of different intercalation agents (nitrogen methylpyrrolidone (NMP), nitrogen nitrogen dimethylformamide (DMF), etc. to obtain liquid mixtures with different ratios of GeAsP/g-C_3N_4. The mixture was subjected to continuous exfoliation in a KM-1000GYT (KSMM, China) ultrasonic instrument for 8 h. Subsequently, the supernatant was collected after centrifugation at 2000 rpm for 10 minutes. This supernatant was then further centrifuged at 8000 rpm for 10 minutes,

and the resulting precipitate was collected. The precipitate was redispersed in an ethanol solution and sonicated for an additional 4 hours to obtain the GeAsP/g-C_3N_4 heterostructure. Finally, the product was collected by centrifugation at 8000 rpm for 10 minutes. To ensure a clean surface, the precipitate was redispersed in ultrapure water and ultrasonically washed. This washing procedure was repeated 3 times. After drying at 80°C for 6 h in a vacuum oven, the GeAsP/g-C_3N_4 heterojunction photocatalysts were obtained. The dried material was ground into a fine powder, stored for subsequent use.

3. Characterizations

The microstructures and morphologies of the as-prepared photocatalysts were characterized using scanning electron microscopy (SEM; MIRA4 LMH, TESCAN, Czech) and transmission electron microscopy (TEM; Talos F200X, FEI, USA). The phase analysis and crystalline quality of the crystal was examined by X-ray diffraction (XRD) with scanning angle from 5 to 80° (Bruker-D8 Discover, Germany). Raman measurements were tested on a Renishaw inVia Reflex spectrometer (inVia Qontor, Britain) using a 532 nm laser. The surface elemental compositions and valence states were investigated by X-ray photoelectron spectroscopy (XPS, ThermoFischer, ESCALAB Xi^+, USA). Photoluminescence (PL) decay profiles were acquired on an ultrafast lifetime spectrofluorometer (Edinburgh FLS1000, Britain) with an

excitation wavelength of 375 nm. Optical absorption characteristics of all the catalysts were measured by UV-vis diffuse reflectance spectra (UV-vis DRS, Shimadzu UV-3600i Plus, Japan). AFM was used to investigate the thickness of samples (Bruker Dimension Icon, Germany). Temperature programmed desorption (TPD, BSD-Chem C20, China) was employed to study the CO_2 adsorption performance.

4. Photocatalytic CO_2 reduction

The photocatalytic activity of the prepared samples was evaluated by measuring their CO_2 reduction performance under visible light irradiation. In a typical procedure, 50 mg of the as-synthesized GeAsP-CN composite photocatalyst powder was dispersed in 45 mL of ultrapure water and 5 mL of triethanolamine (TEOA) within a photocatalytic reactor (CEL-APR100H Photochemical Temperature-Controlled All-in-One Reactor, China, Fig. S1). The suspension was purged with high-purity CO_2 gas for 30 minutes in the dark to establish an adsorption-desorption equilibrium. Throughout the reaction, the temperature was maintained at 298 K using a circulating cooling water system and ensure that temperature fluctuations were less than 5 K during the reaction, and the mixture was continuously stirred with a magnetic stirrer. A 300 W Xenon lamp (Microsolar300, Perfectlight, China) equipped with a 420 nm cut-off filter served as the visible light source to initiate the photoreduction. At 1-hour intervals, 100 μL of gas was sampled from the reactor headspace.

The concentrations of carbon monoxide (CO) and methane (CH_4) were then analyzed using a Shimadzu GC-2010 gas chromatograph equipped with a flame ionization detector (FID).

The apparent quantum yields (AQY) were measured using monochromatic LED lamps (420 nm and 520 nm) to evaluate the wavelength-dependent photocatalytic activity. The incident light power intensity was determined using a handheld solar power meter (SM206E-solar). The AQY was calculated according to the following equation:

$$AQY = \frac{2N(CO) + 8N(CH_4)}{\frac{P \times S \times t \times \lambda}{h \times c}}$$

where *N(CO)* and *N(CH_4)* represent the molar amounts of the evolved products (CO and CH_4, respectively), assuming a 2-electron and 8-electron reduction process. *P* is the light power density, *S* is the irradiation area, *t* is the reaction time, λ is the monochromatic wavelength, *h* is Planck's constant, and *c* is the speed of light.

5. Photoelectrochemical measurements

Photoelectrochemical measurements were performed on a CHI 760E electrochemical workstation (Fig. S2) using a standard three-electrode configuration with as-prepared catalyst coated on FTO glass (1×1 cm^2), Ag/AgCl (saturated KCl) and Pt wire as the working electrode, reference electrode and counter electrode, respectively. All measurements were conducted in a CO_2-saturated 0.5 M Na_2SO_4 aqueous solution containing 20 vol% TEOA as a sacrificial agent. A 300 W Xe arc lamp with a UV

light cut-off filter ($\lambda > 420$ nm) was taken as a light source. Electrochemical impedance spectroscopy (EIS) was conducted at the open-circuit potential (OCP) under both dark and illuminated conditions, scanning from 10^5 Hz to 0.1 Hz with a 1 mV amplitude. Transient photocurrent responses were measured at OCP by switching the light on and off at 5 s intervals. Mott-Schottky plots were obtained in the dark at a fixed frequency of 1.5 kHz with a perturbation amplitude of 5 mV.

Fig. S1. Optical image of photocatalytic reactor

Fig. S2. Optical image of a three electrode photoelectrochemical measuring device

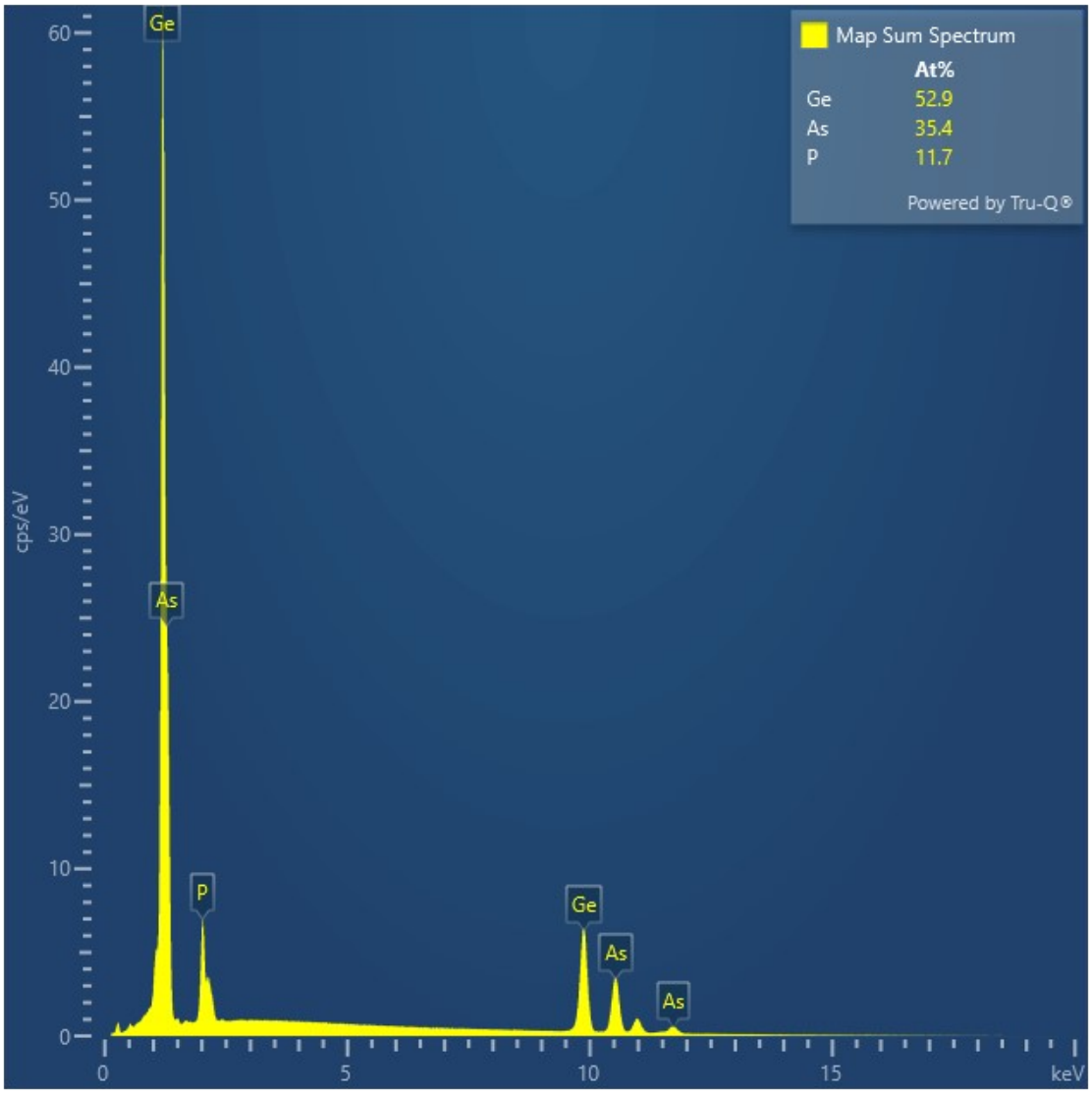

Fig. S3. SEM-EDS spectra of the GeAsP

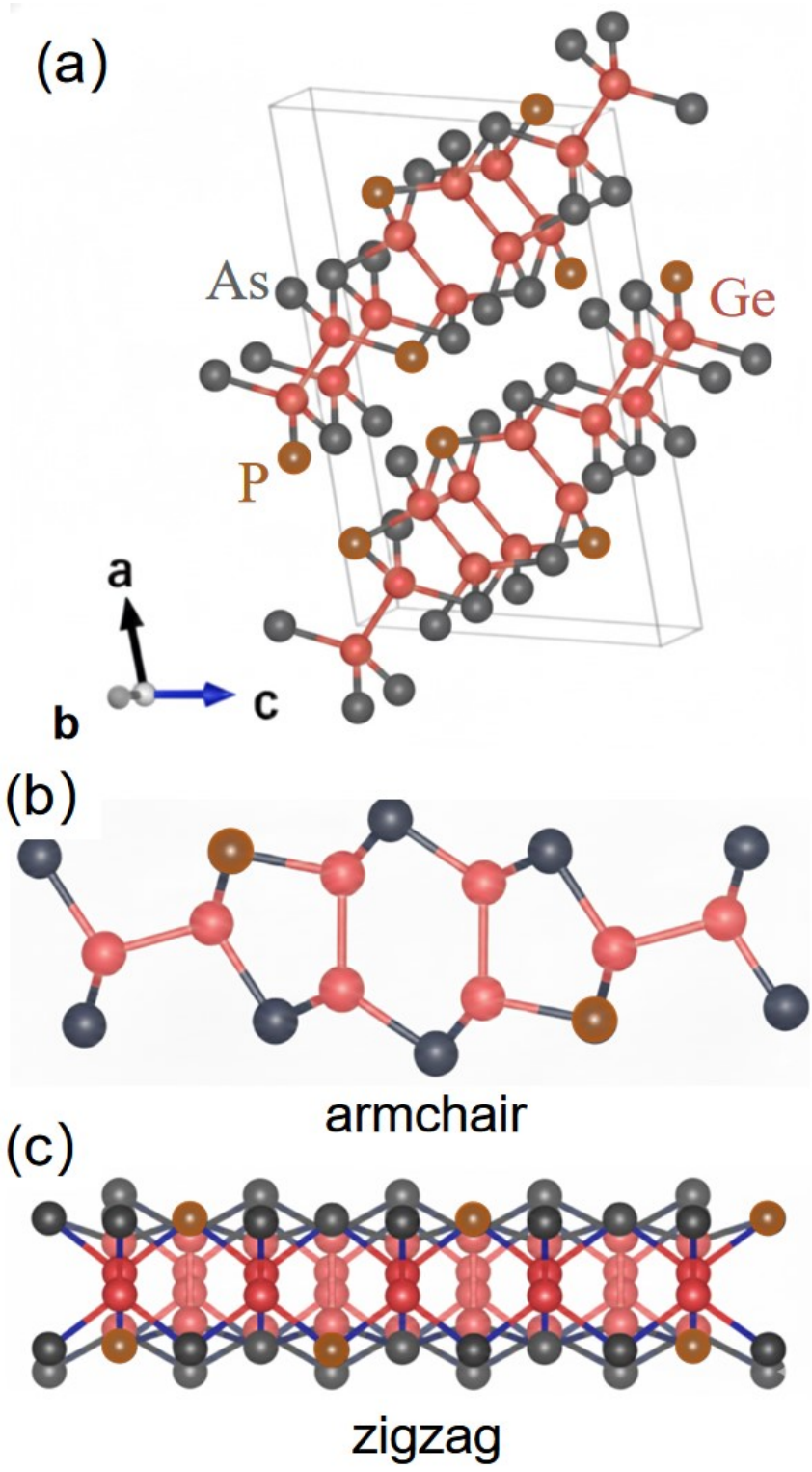

Fig. S4. (a) Crystal structure diagram of GeAsP, atomic structure diagram of GeAsP in the (b) armchair and (c) zigzag directions

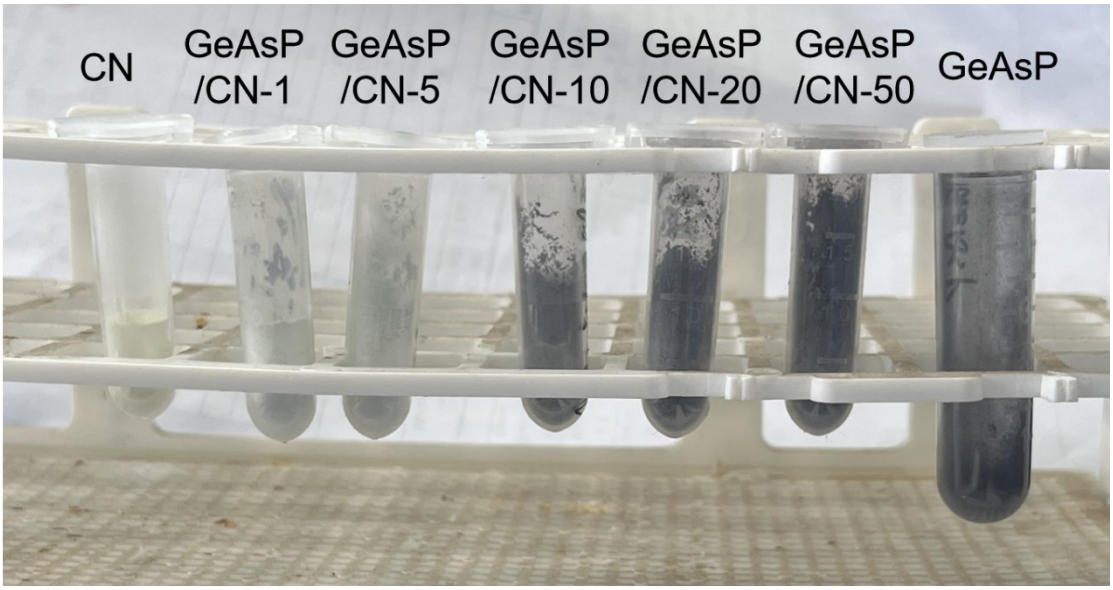

Fig. S5. Optical images of CN, GeAsP and GeAsP/CN-X (X represents x% of b-AsP, compared to CN)

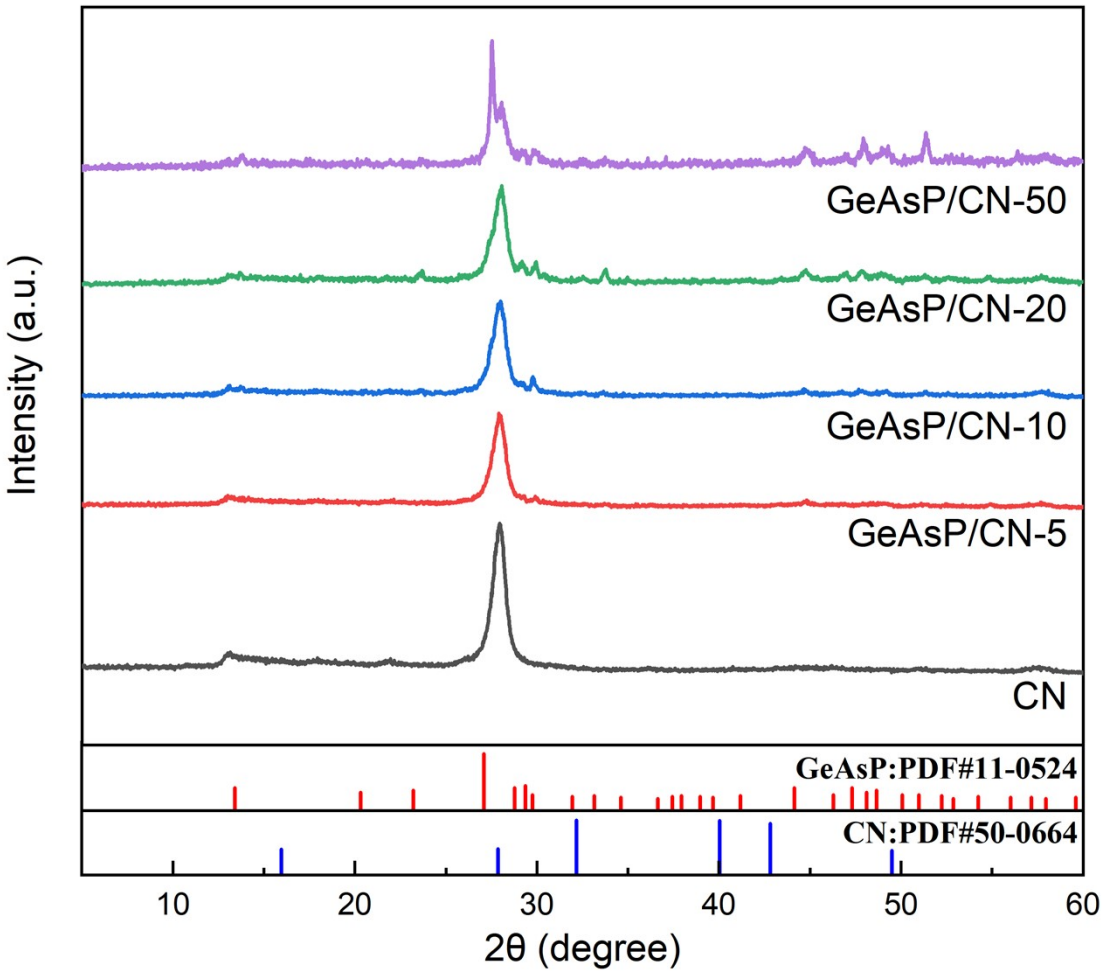

Fig. S6. XRD patterns of CN and GeAsP/CN-X

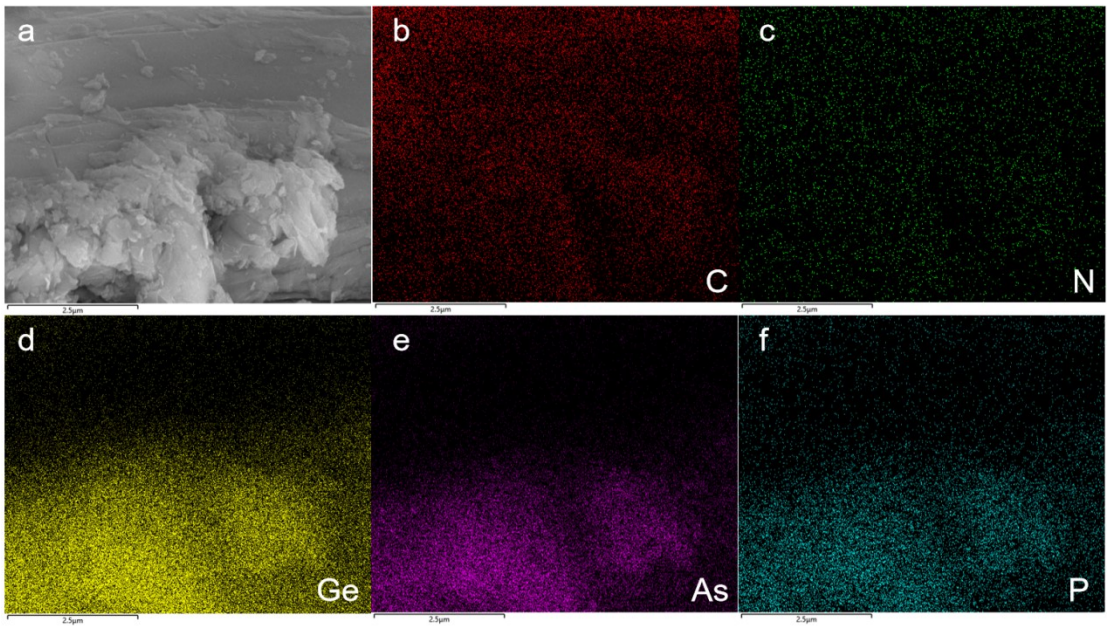

Fig. S7. SEM and SEM-EDS mapping images of the GeAsP/CN-20

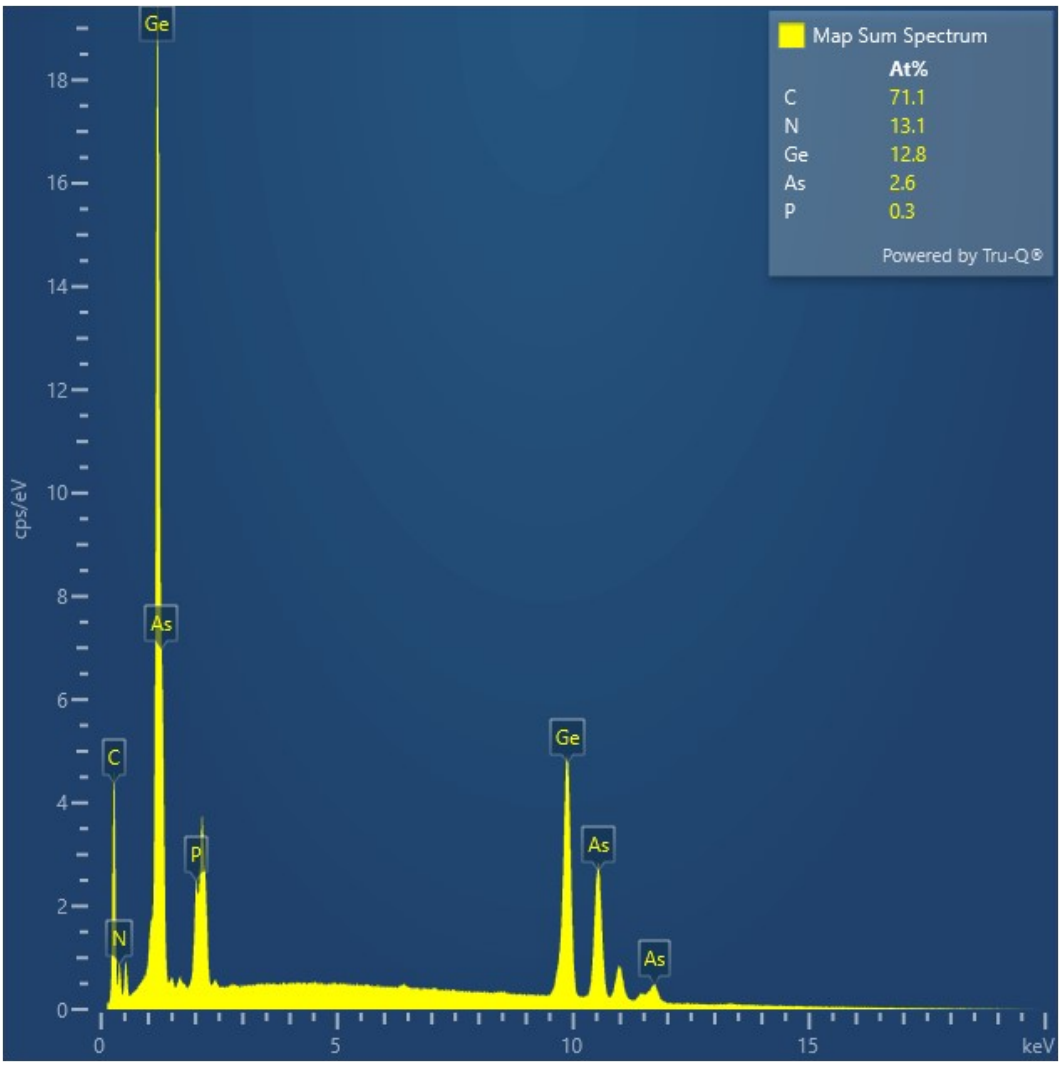

Fig. S8. SEM-EDS spectra of the GeAsP/CN-20

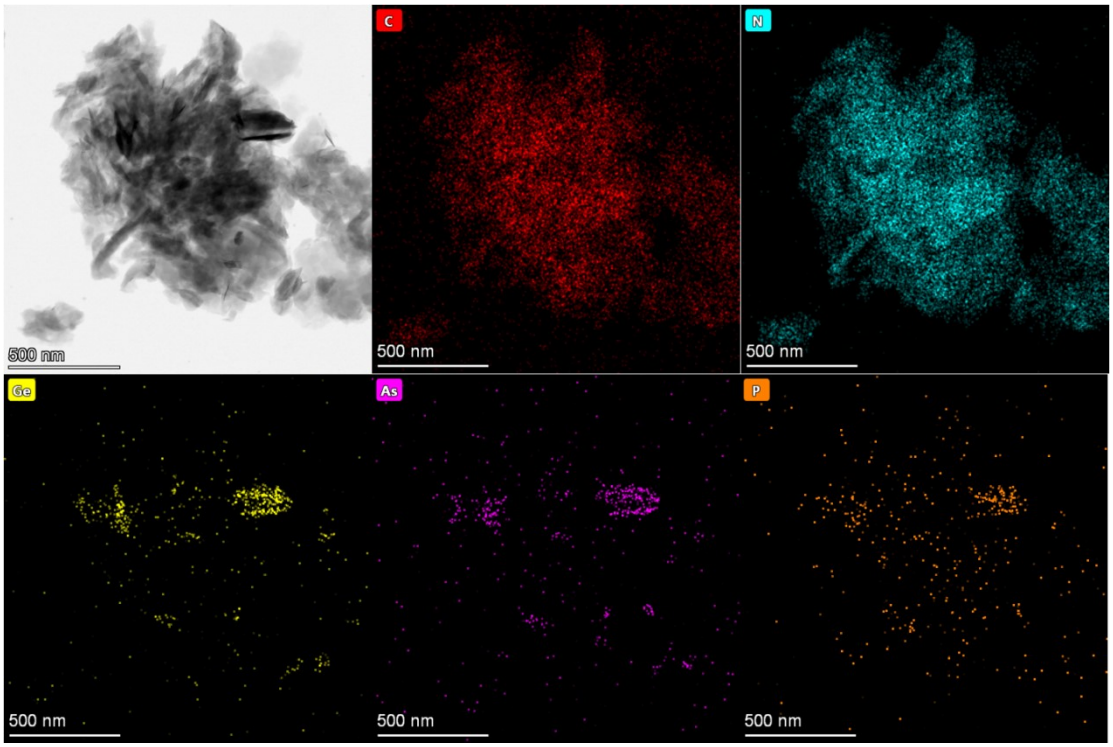

Fig. S9. TEM and TEM-EDS mapping images of the GeAsP/CN-20

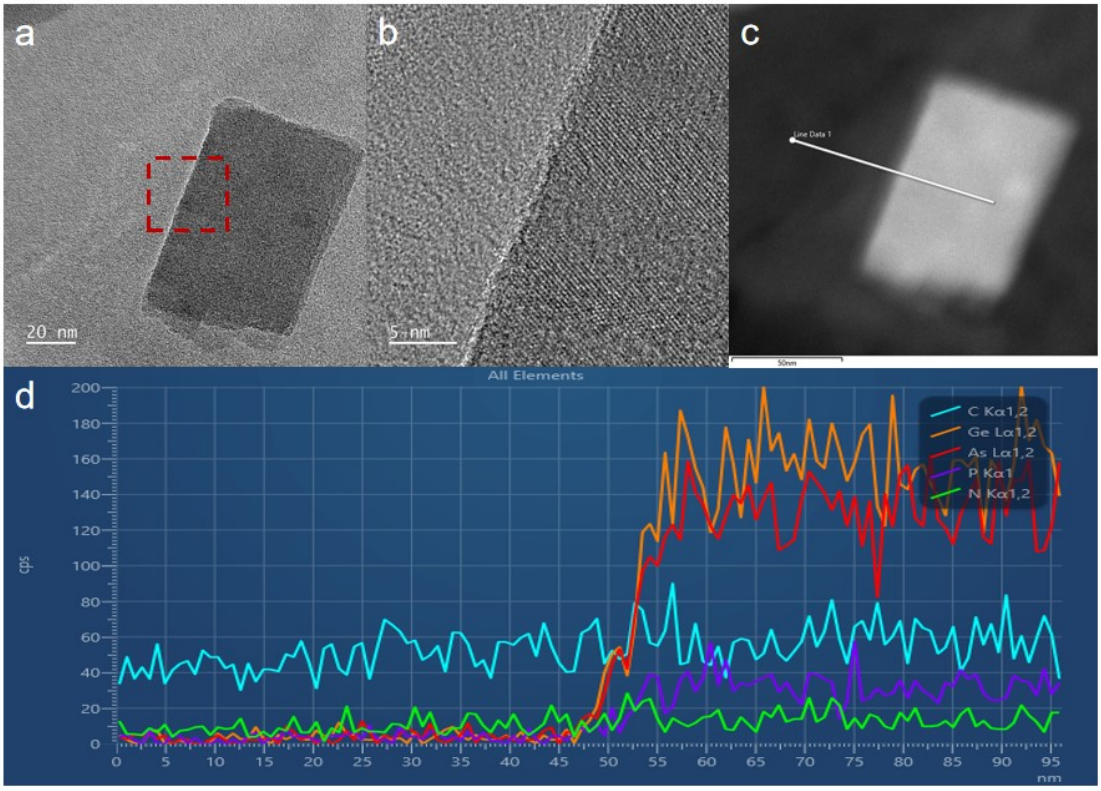

Fig. S10. (a-b) HRTEM image of CN and GeAsP combined interface. (c) TEM-EDS line scan images and (d) result statistics of CN and GeAsP combined interface

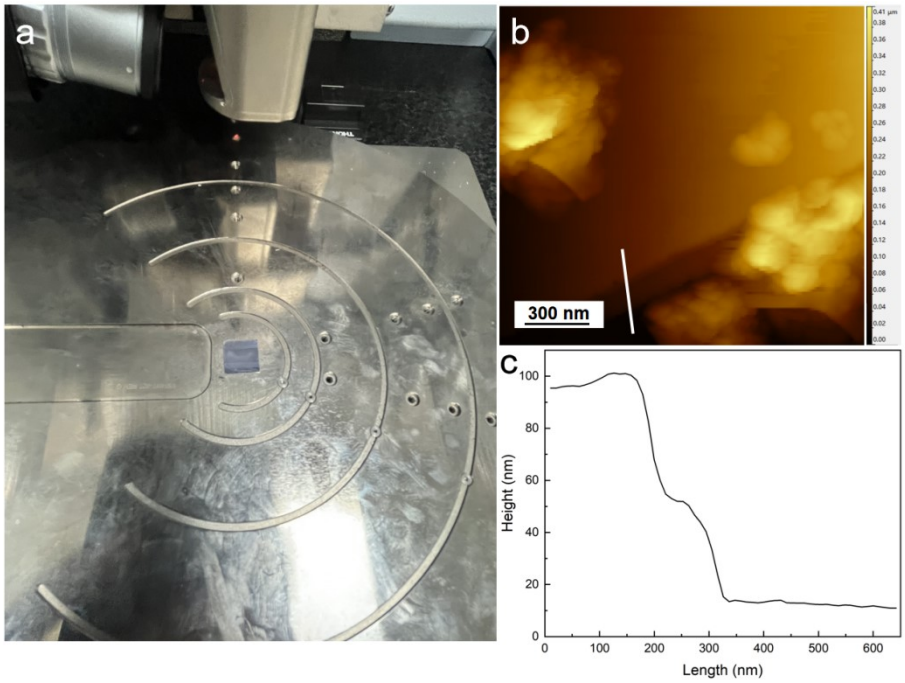

Fig. S11. (a) Optical photos, (b) AFM results and (c) AFM height statistics of GeAsP/CN-20 material spin coated on a SiO_2 substrate

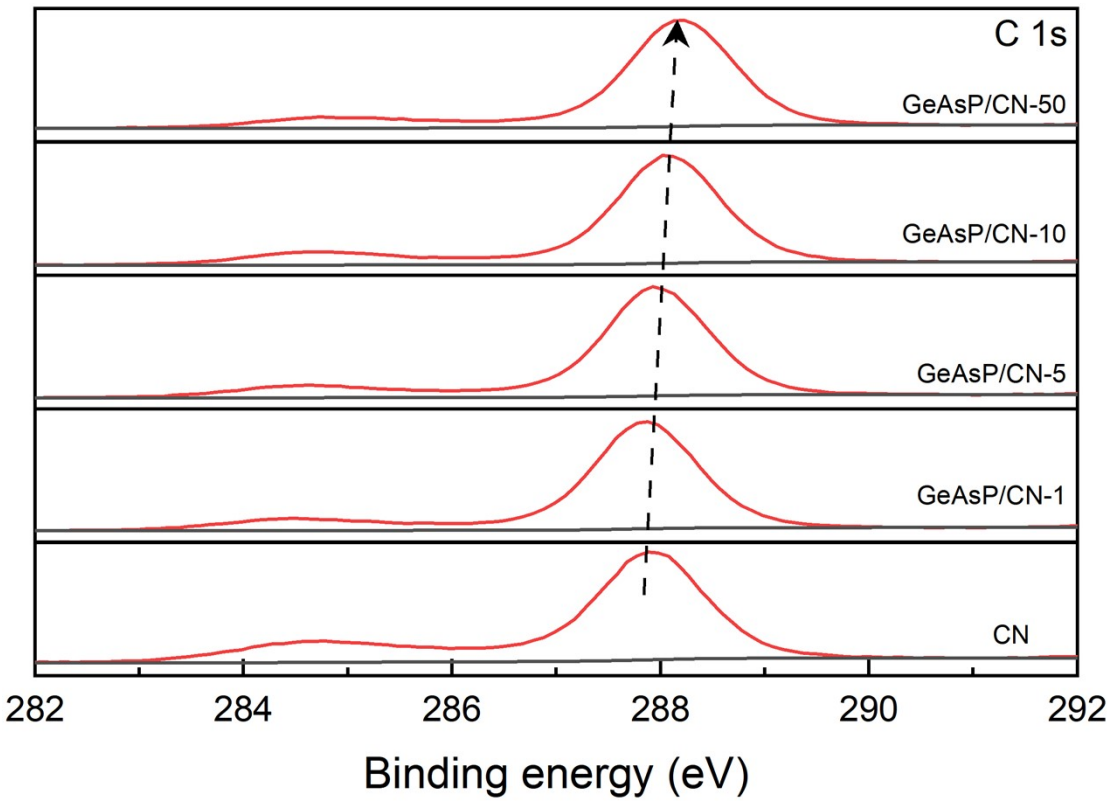

Fig. S12. XPS spectra of C 1s in CN and GeAsP/CN-X

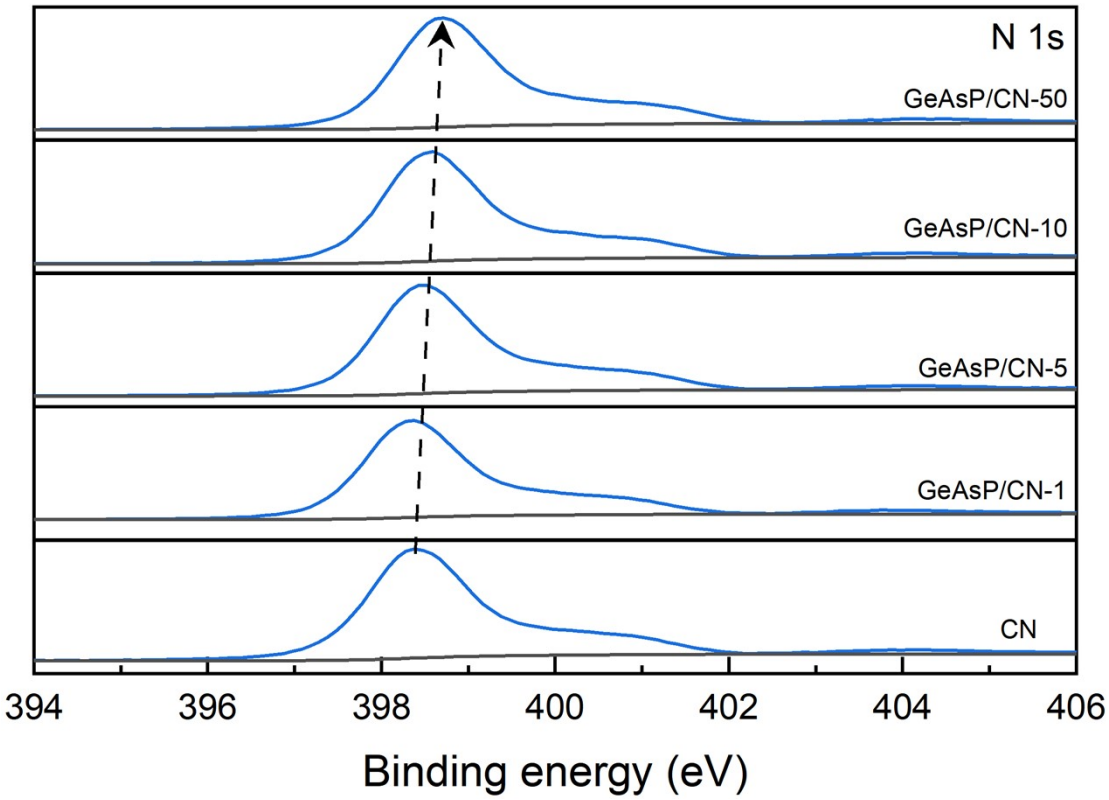

Fig. S13. XPS spectra of N 1s in CN and GeAsP/CN-X

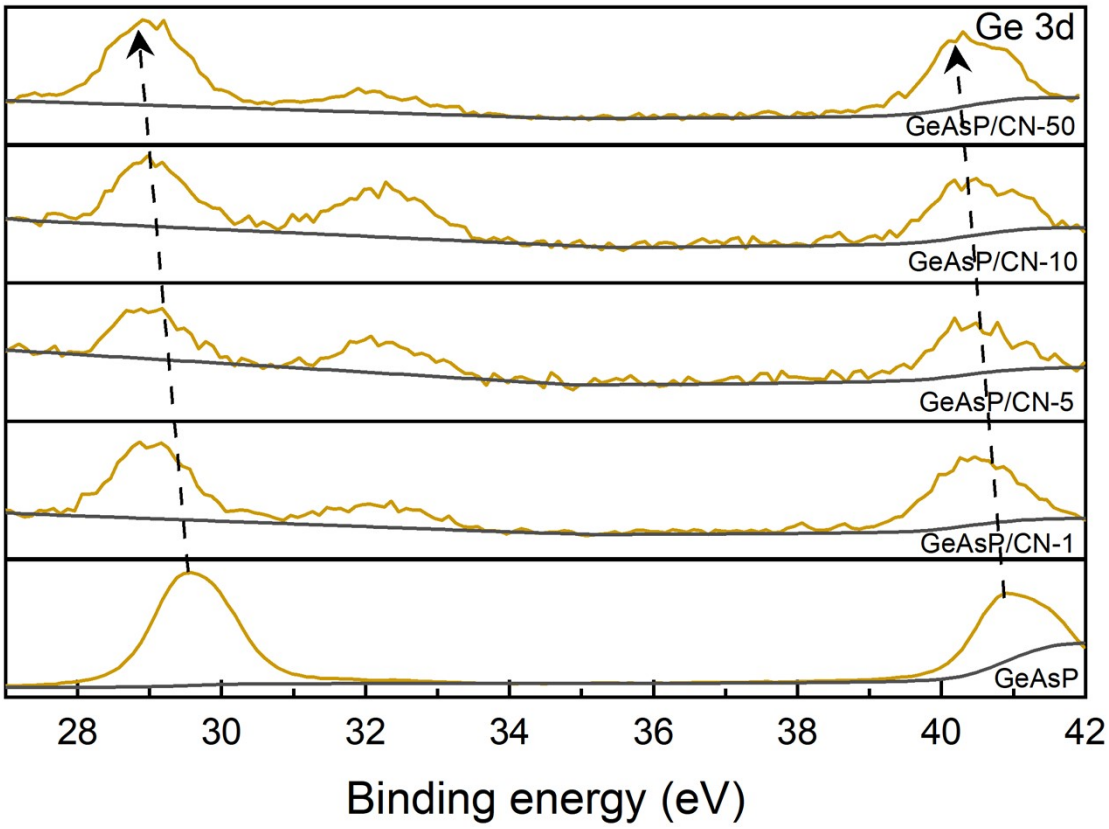

Fig. S14. XPS spectra of Ge 3d in b-AsP and GeAsP/CN-X

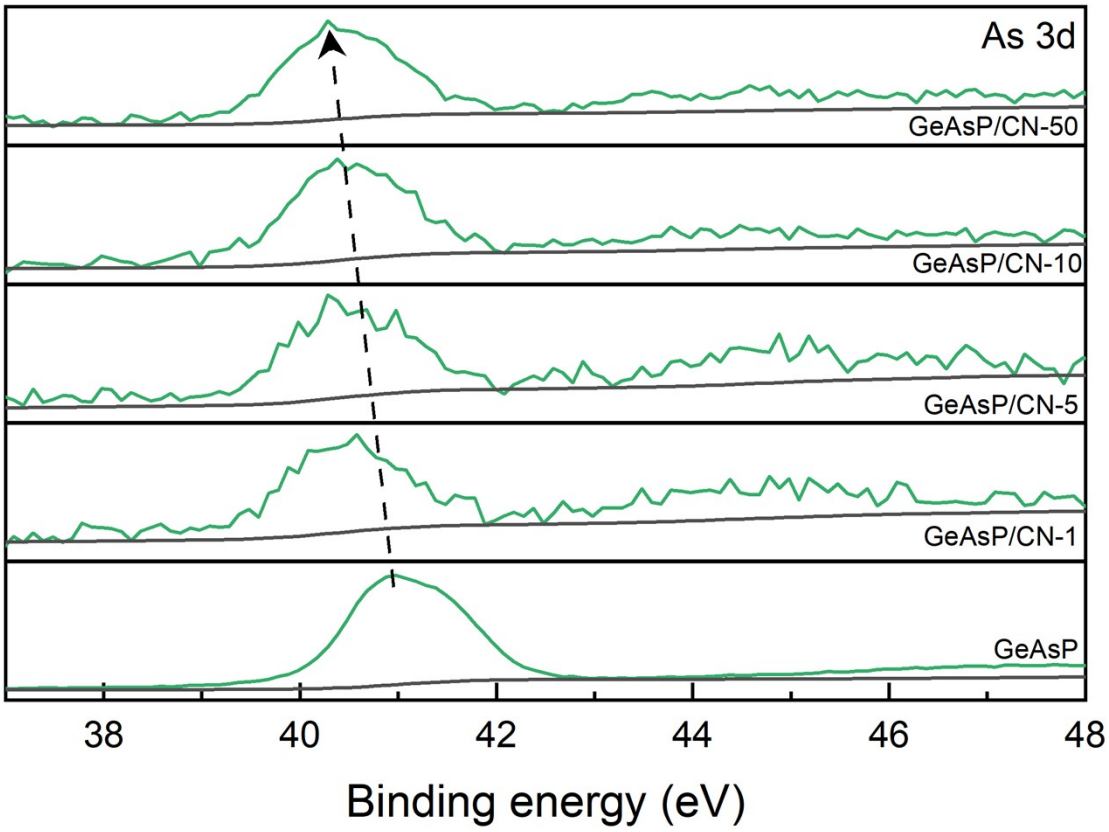

Fig. S15. XPS spectra of As 3d in b-AsP and GeAsP/CN-X

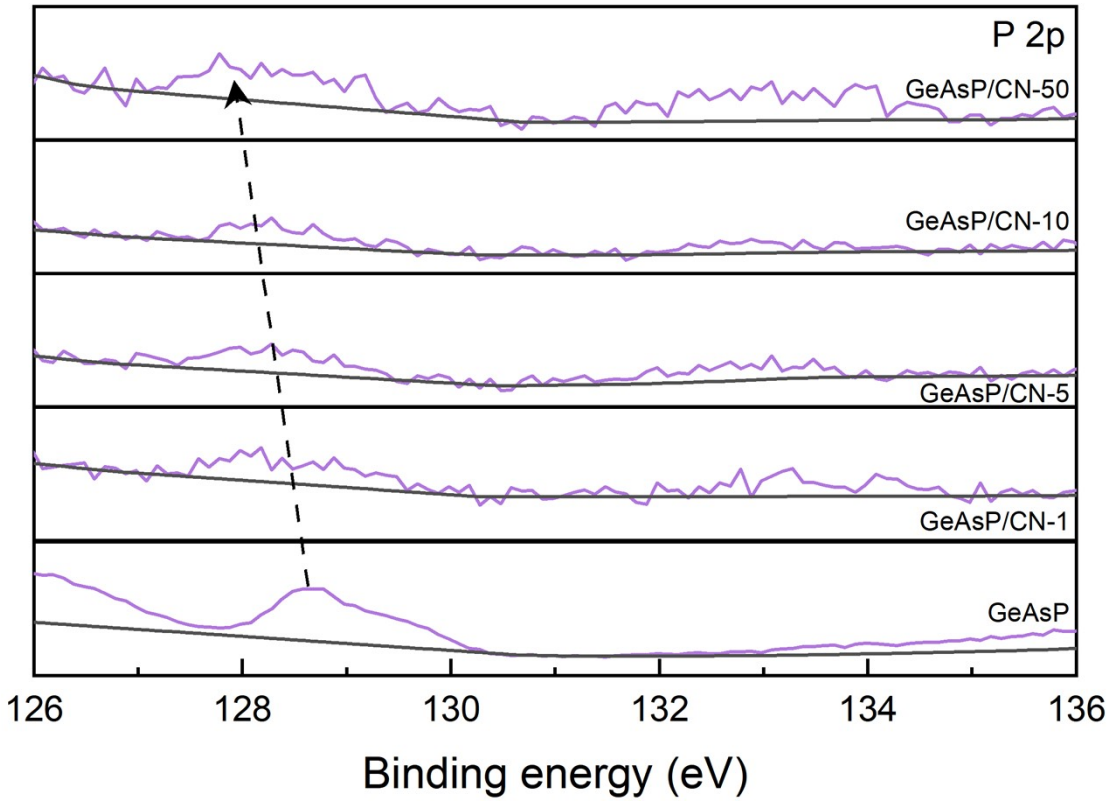

Fig. S16. XPS spectra of P 2p in b-AsP and GeAsP/CN-X

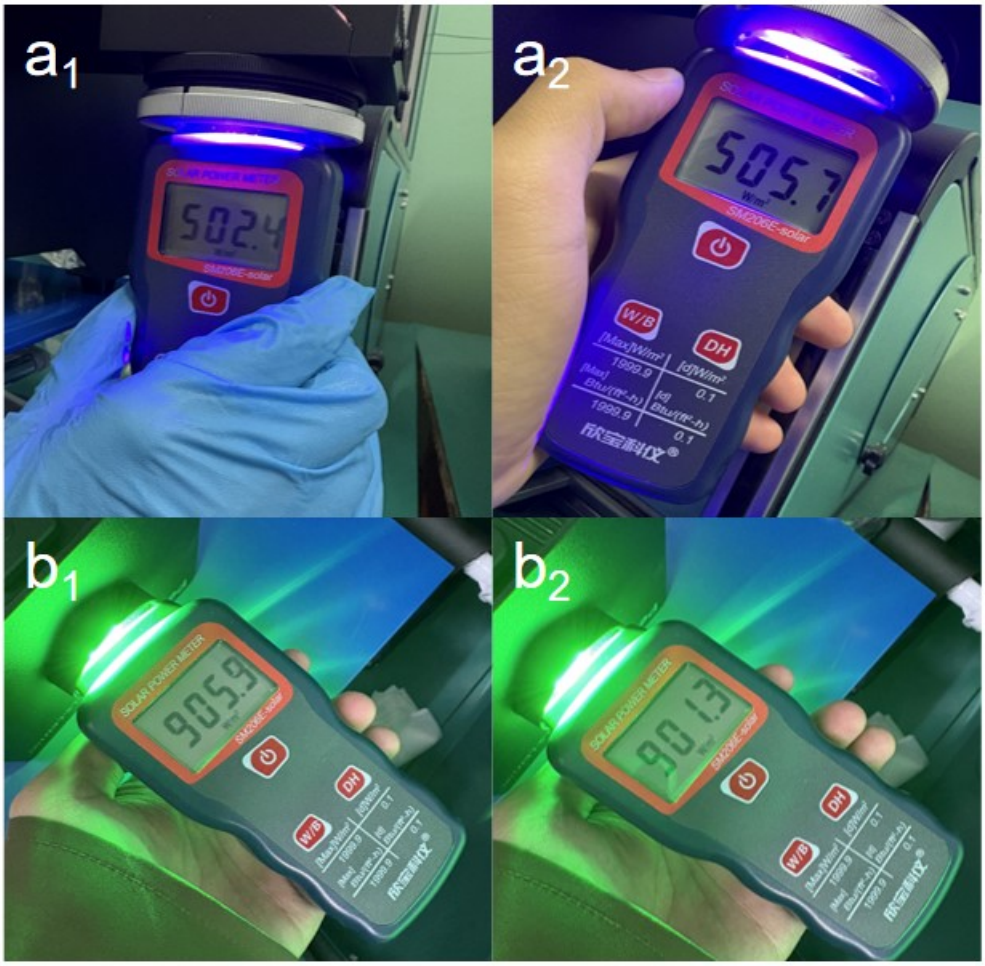

Fig. S17. Photo of the measurement process of incident light power during single wavelength (a: 420 nm, b: 520 nm) testing

Tab. S1. The apparent quantum efficiency of photocatalysts at different single wavelengths

Photocatalyst	Light source (nm)	light power density	AQY (%)
GeAsP-20	420	504.1	1.28
	520	903.6	0.16

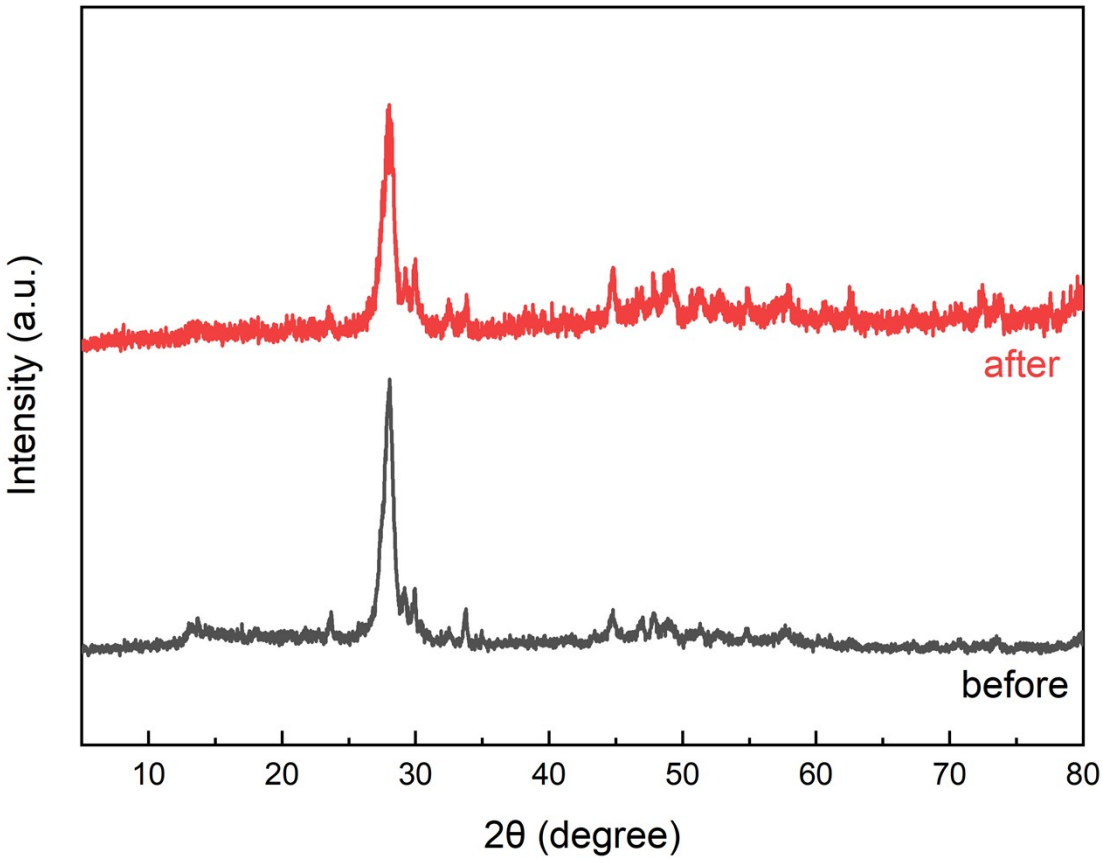

Fig. S18. XRD comparison of the GeAsP/CN-20 before and after use

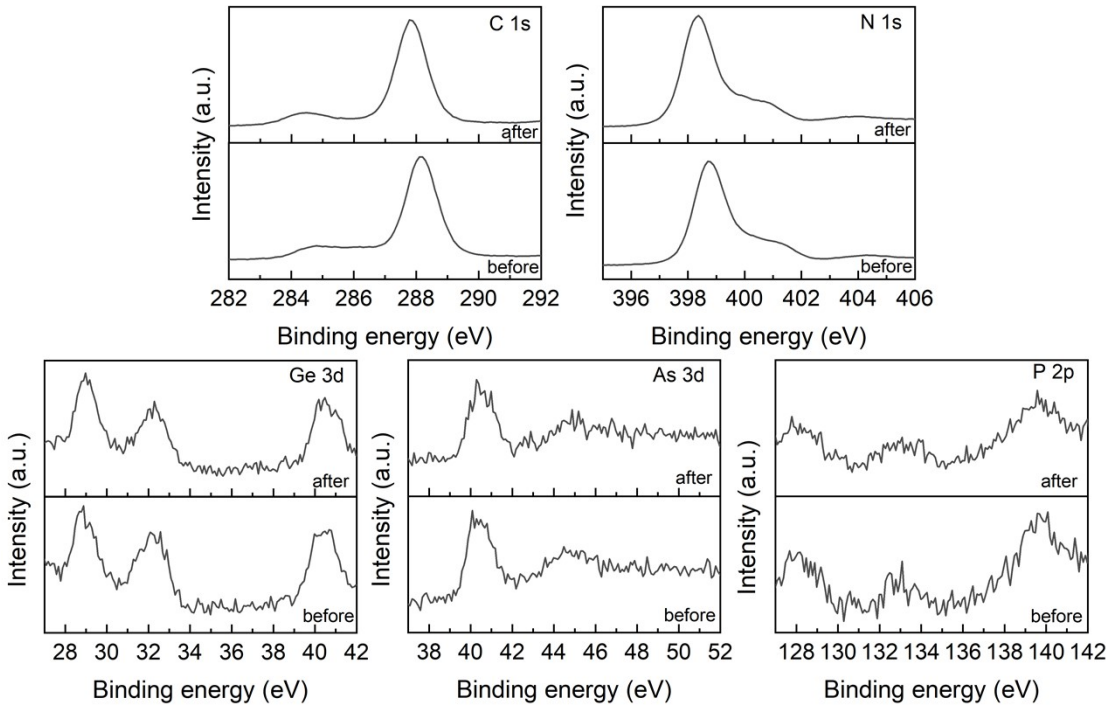

Fig. S19. XPS comparison of the GeAsP/CN-20 (a) before and (b) after use

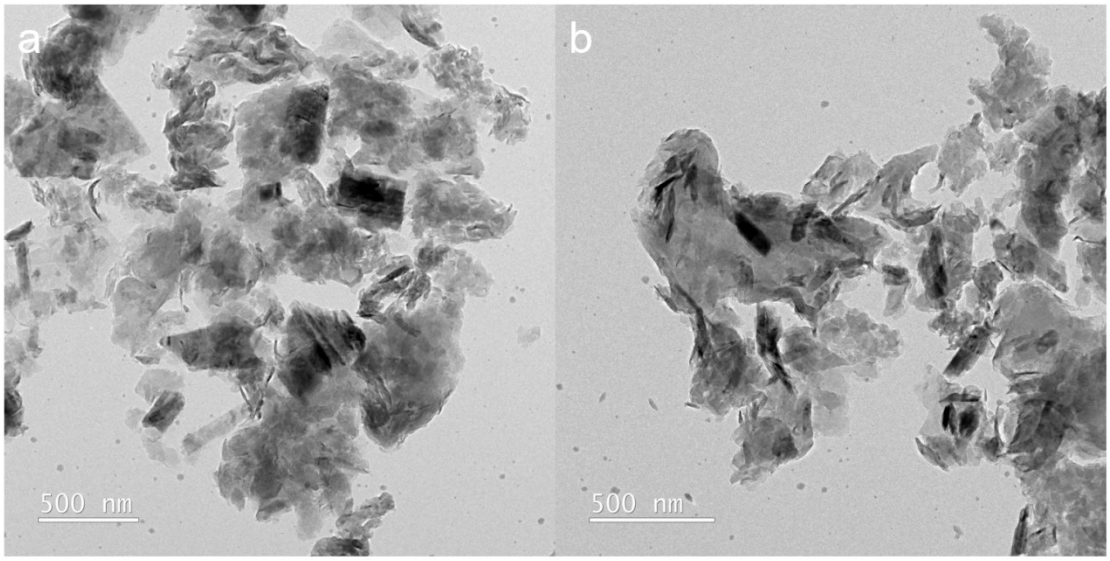

Fig. S20. TEM comparison of the GeAsP/CN-20 (a) before and (b) after use

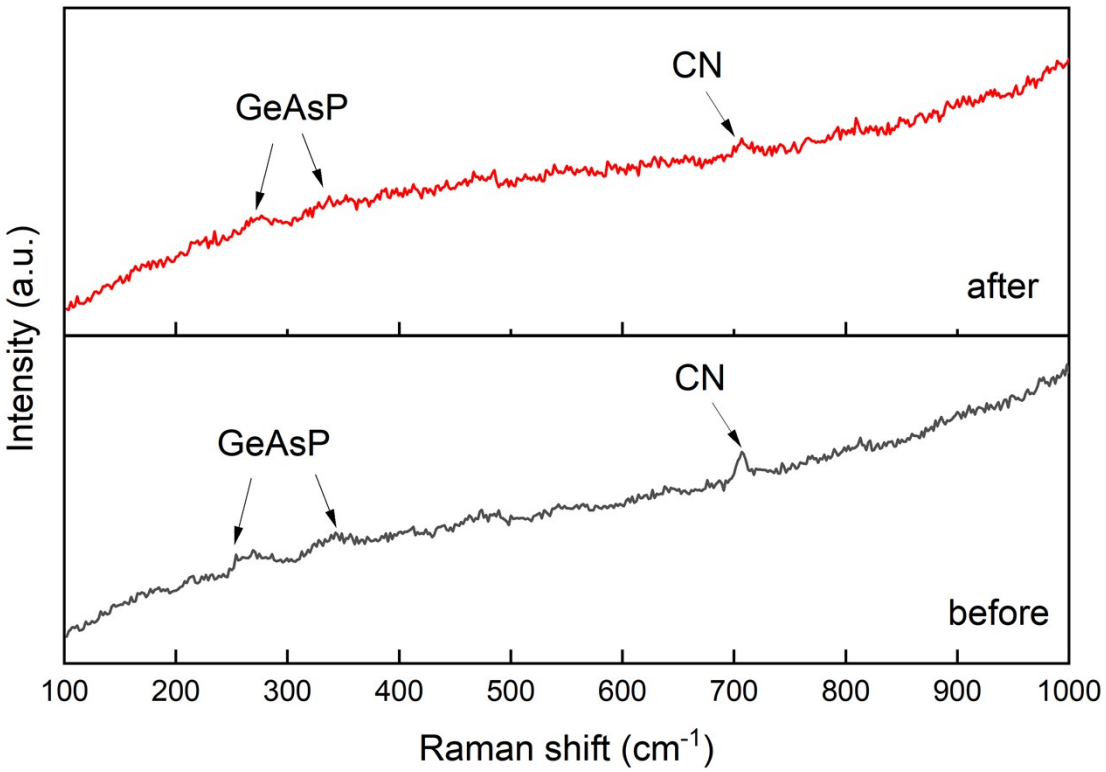

Fig. S21. Raman comparison of the GeAsP/CN-20 (a) before and (b) after use

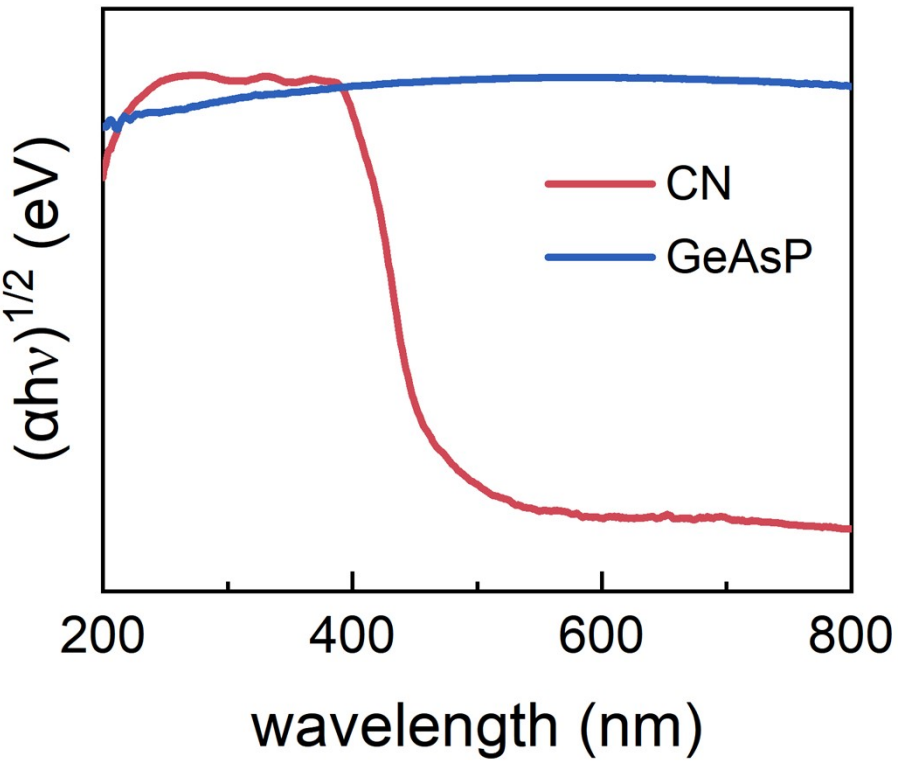

Fig. S22. (a) UV-vis spectroscopy of CN and GeAsP

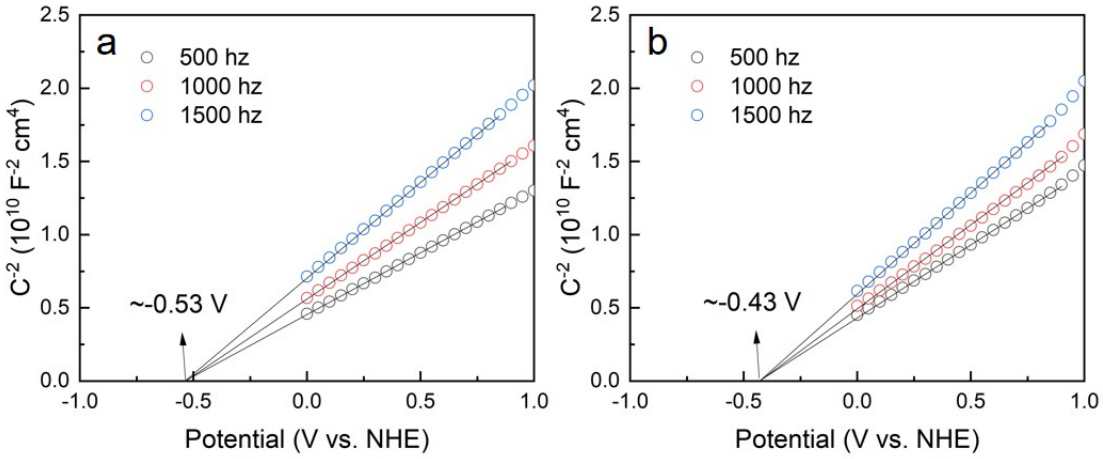

Fig. S23. The Mott-Schottky plots of (a) CN and (b) GeAsP

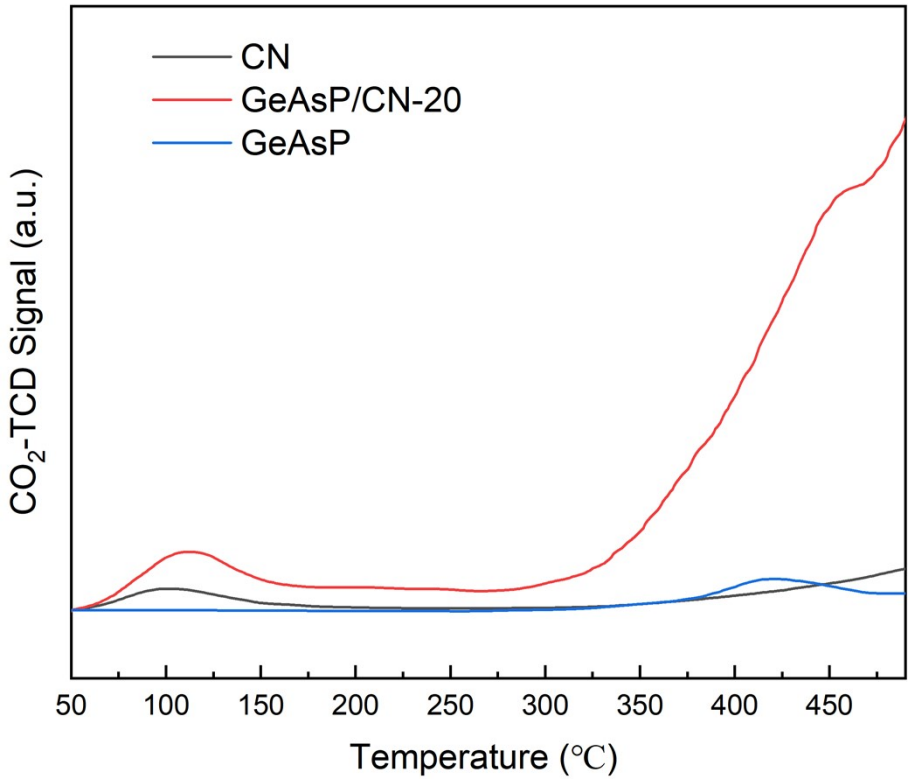

Fig. S24. CO_2-TPD patterns (normalized per unit mass) for the CN, GeAsP/CN-20 and GeAsP

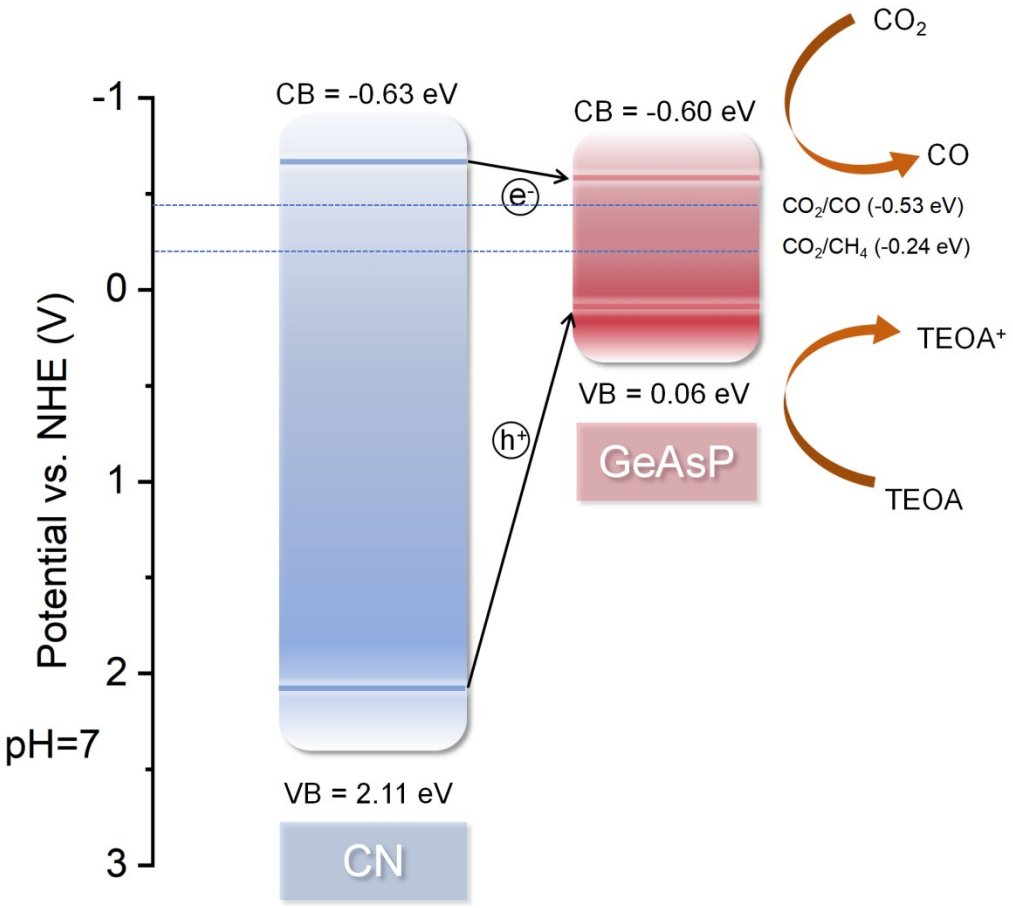

Fig. S25. Schematic diagram of the photocatalytic mechanism of 2D GeAsP/CN system under visible-light irradiation